Magnetic Structures of Holmium. I. The Virgin State*

W. C. KOEHLER, J. W. CABLE, M. K. WILKINSON, AND E. O. WOLLAN
Solid State Division, Oak Ridge National Laboratory, Oak Ridge, Tennessee
(Received 1 June 1966)

Neutron-diffraction measurements have been made on single-crystal specimens of holmium at temperatures ranging from room temperature to 4.2°K. Below the Néel temperature of 133°K, the moments order in a helical structure in which the c axis is the screw axis. The interlayer angle varies from about 50° per layer at T_N to 30.0° per layer at 4.2°K. Below about 20°K the structure is a conical configuration in which there is a net moment of $1.7\mu_B$ parallel to the c axis. The configuration of moments in the basal plane at 4.2°K is a distorted helical one in which moments of $9.5\mu_B$ are bunched around the easy b directions in the plane.

INTRODUCTION

THE physical properties of metallic holmium exhibit a number of anomalies which are now known to be related to the magnetic properties of the metal. Thermal measurements[1] on polycrystalline holmium have revealed two strong peaks in the specific-heat–versus–temperature curve: a λ-type anomaly occurs at 131.4°K, and a smaller, symmetrical, history-dependent peak is found at 19.4°K. Magnetic measurements on polycrystalline holmium in the paramagnetic region[2,3] show that the atoms behave, to a good approximation, as tripositive ions, i.e., that they have effective moments close to the value of $10.6\ \mu_B$ per atom expected for the $^5I_8$ spectroscopic state. At lower temperatures[2] the magnetic measurements show strong evidence for a magnetic-ordering transition to an antiferromagnetic state at a temperature near that of the λ anomaly and for a second transition to a ferromagnetic state at about 20°K. Results of magnetization measurements on single-crystal specimens have demonstrated that the magnetization process in the metal is extremely complicated.[4] There is observed a very pronounced hexagonal anisotropy of the magnetization as well as a very considerable axial anisotropy. Even in the paramagnetic region, the paramagnetic Curie points measured with the field parallel or perpendicular to the c axis of the hexagonal-close-packed structure differ significantly.

The results of rather extensive neutron-diffraction studies designed to investigate the microscopic magnetic properties of metallic holmium have, up to now, been described only partially and in several brief and widely scattered communications.[5–7] In this paper we present a complete report of the results of experiments carried out on the metal in the virgin state. Other aspects of the investigations will be dealt with in separate publications.

EXPERIMENTAL

The earliest neutron-diffraction data for holmium were obtained with polycrystalline specimens. However, in the course of examining samples of different origin, a large grain was found in a cast rod of Ames metal. From this grain a single crystal was ultimately isolated and extensively studied. This crystal, to which we refer as Ho(A), was approximately disk-shaped, 5 mm in diameter and 1 mm thick and had its c axis at an angle of 45° to the surface of the disk. A second crystal, obtained much later, was extensively studied also. This specimen, Ho(B), was cut from a piece of a large single crystal grown at Ames by the strain-anneal method. It was accurately disk-shaped, 5 mm in diameter, 2 mm thick, and had its c axis normal to the plane of the disk. The bulk of the data was obtained with these two crystals, although shorter studies were made with several other crystals of different size and shape, and with polycrystalline samples of various degrees of purity.[8]

The single-crystal specimens were maintained in one of the ORNL low-temperature goniometers in such a way that the c axis of the crystal was parallel to the horizontal rotation axis of the instrument. Systematic surveys of important regions of reciprocal space were made at various appropriate temperatures between 4.2°K and room temperature. For the irregularly shaped specimen, Ho(A), absorption corrections were made experimentally and the magnetic intensities placed on an absolute basis by comparison with the nuclear intensities in a manner similar to that described in an earlier paper.[9] For Ho(B) absorption corrections were

* Research sponsored by the U. S. Atomic Energy Commission under contract with the Union Carbide Corporation.

[1] B. C. Gerstein, M. Griffel, L. D. Jennings, and R. E. Miller, J. Chem. Phys. **27**, 394 (1957).

[2] B. L. Rhodes, S. Legvold, and F. H. Spedding, Phys. Rev. **109**, 1544 (1958).

[3] S. Arajs and R. V. Colvin, in *Rare Earth Research*, edited by Eugene Kleber (The Macmillan Company, New York, 1961), p. 178.

[4] D. L. Strandberg, S. Legvold, and F. H. Spedding, Phys. Rev. **127**, 2046 (1962).

[5] W. C. Koehler, E. O. Wollan, M. K. Wilkinson, and J. W. Cable, in *Rare Earth Research*, edited by Eugene Kleber (The Macmillan Company, New York, 1961), p. 149.

[6] W. C. Koehler, J. Appl. Phys. **32**, 20S (1961).

[7] W. C. Koehler, J. W. Cable, E. O. Wollan, and M. K. Wilkinson, J. Phys. Soc. Japan Suppl. **17**, 32 (1962).

[8] The crystal Ho(B) was obtained for a study of the magnetization process of Ho. During preliminary orientation and exploratory measurements with it, it was noted that it differed in some respects from Ho(A). The main features of the magnetic structures of holmium as deduced from the two crystals are identical, however, and we do not distinguish the two except where we specifically wish to emphasize the differences in structural detail in the two cases. The cause for the difference is thought to be due to strain in Ho(A). See Appendix.

calculated as well with the Busing and Levy program.[10] Debye-Waller corrections were made with a characteristic temperature of 161°K.[1] Except for the very strong magnetic satellite reflections of the origin of reciprocal space, extinction did not appear to be a serious problem in these crystals.

RESULTS

1. The High-Temperature Form

As the crystal was cooled below the Néel temperature, magnetic reflections were observed as satellites of the nuclear reflections. The data characteristic of holmium in the range between 20°K and T_N are illustrated in Fig. 1 where a rocking curve about the (100) reflection at a sample temperature of 77°K is shown. The insert, a portion of reciprocal space, illustrates the procedure and the scheme adopted for identifying the satellites.

The full circles in the diagram are supposed to represent nuclear scattering: No circle is indicated at (001) because that reflection is forbidden. Magnetic satellites are found symmetrically arranged about each allowed nuclear reflection, including the origin, and these are located on lattice rows parallel to the reciprocal lattice vector $\mathbf{b}_3$. The positions of the satellites do not necessarily conform to any simple multiplicity of chemical unit cell dimensions; moreover the separation of a satellite from its associated lattice point changes continuously with temperature.

The occurrence of such satellite reflections shows that the periodicity of the ordered magnetic moment is different from that of the distribution of atoms. In addition the existence of a single pair of satellites around allowed lattice points implies that the Fourier series which represents the moment distribution possesses but one term, the fundamental.

TABLE I. Intensities of magnetic reflections of Ho at 77.5°K. The observed $|F|^2$ values, in units of 10^{-24} cm^2, have been averaged over equivalent reflections. In the calculated values $p^2=0.0725$, $\mu^2=3.77$, $\mu=(7.2\pm4)\mu_B$.

Reflection[a]	$\lvert F\rvert_{obs}^2$	$\lvert F\rvert_{calc}^{2}$ [b]
$(100)^-$	0.78±0.04	0.777
$(100)^+$	0.82±0.04	0.777
$(101)^-$	2.46±0.12	2.56
$(101)^+$	2.60±0.13	2.75
$(\bar{1}01)^-$	2.44±0.12	2.56
$(\bar{1}01)^+$	2.66±0.13	2.75
$(102)^-$	0.97±0.10	0.930
$(102)^+$	0.99±0.10	0.882
$(002)^-$	6.02±0.30	6.60
$(002)^+$	5.25±0.26	5.52
$(110)^-$	2.06±0.10	1.98
$(110)^+$	1.94±0.10	1.98
$(11\bar{2})^-$	2.08±0.10	1.91
$(\bar{1}\bar{1}2)^-$	2.00±0.10	1.91
$(\bar{1}\bar{1}2)^+$	1.86±0.10	1.79

[a] Averaged over equivalent reflections.
[b] $\langle p\rangle^2=3.77$, $\mu=7.2\pm0.4$.

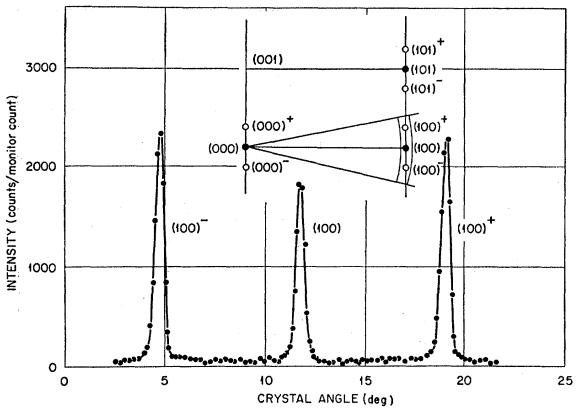

FIG. 1. Rocking curve about the (100) position in Ho at 77°K. The inset shows schematically the experimental procedure for obtaining these data, the indexing scheme adopted for the satellites, and the magnetic scattering density in reciprocal space.

The intensities observed for Ho in the high-temperature range can be well accounted for on the basis of a helical structure. In this model the moments are described by

$$\begin{aligned}\mu_{nx}&=\mu\cos(2\pi\boldsymbol{\tau}\cdot\mathbf{r}_n+\alpha),\\ \mu_{ny}&=\mu\sin(2\pi\boldsymbol{\tau}\cdot\mathbf{r}_n+\alpha),\\ \mu_{nz}&=0,\end{aligned}\qquad(1)$$

where μ is the magnitude of the moment, $\mathbf{r}_n$ is the position vector in the crystal of the nth moment and α is an arbitrary phase angle. The wave vector of the modulation $\boldsymbol{\tau}$ is parallel to the c axis of the crystal and to the reciprocal lattice vector $\mathbf{b}_3$.

In such a structure the moments of the atoms within a given hexagonal layer are parallel to each other. The directions of the moments in adjacent layers make an angle ω with each other given by $\omega=\pi\tau c$.

The structure factors for the helical structure are given by

$$|F|_{hkl^{\pm}}^2=0.0725[(1+\cos^2\phi)/4]\mu^2f^2|G^2|_{hkl},\qquad(2)$$

in which ϕ is the angle between the scattering vector $\mathbf{s}^{\pm}$ of the satellite [$\mathbf{s}^{\pm}=2\pi(B_H+\boldsymbol{\tau})$, $\mathbf{B}_H$=a reciprocal lattice vector] and the screw axis, f is the magnetic form factor, and $|G|_{hkl}$ is the geometrical structure factor for the reflection (hkl). In Eq. (2) the magnetic moment μ is to be expressed in Bohr magnetons.

A comparison of values of $|F|_{hkl^{\pm}}^2$ observed for Ho at 77°K, and those calculated from Eq. (2), is given in Table I. The angle ϕ is derived from a knowledge of the chemical unit cell dimensions and of the magnitude of the interlayer turn angle which was measured independently. For the first stages of the calculation the Ho^{+3} ion form factor deduced from paramagnetic-

[9] W. C. Koehler, J. W. Cable, E. O. Wollan, and M. K. Wilkinson, Phys. Rev. **126**, 1672 (1962).
[10] W. R. Busing and H. A. Levy, Acta Cryst. **10**, 180 (1957).

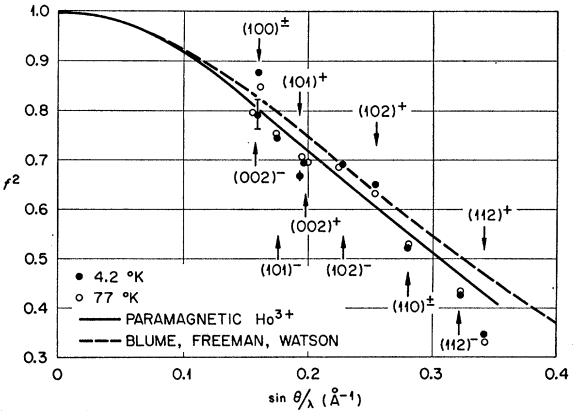

FIG. 2. Form-factor data for metallic holmium. Form-factor data as derived from single-crystal measurements at 77°K (open circles), 4.2°K (full circles), and from paramagnetic scattering by polycrystalline Ho_2O_3 (solid curve) are compared with the theory (dashed curve). The data are presented as f^2 versus $\sin\theta/\lambda$.

scattering measurements on Ho_2O_3 [11] was assumed and a preliminary value of the average moment was derived. Successive iterations produced little change in the moment value, but some modification of the form factor for larger scattering angles was required.

The agreement between observed and calculated values of $|F|_{hkl\pm}^2$ appears to be quite satisfactory. The final form-factor data derived from the 77°K data, and from data, to be discussed below, taken at 4.2°K are presented in Fig. 2. The solid curve is the experimental form factor from the paramagnetic scattering from Ho_2O_3 and the dashed curve is a theoretical curve obtained from Trammell's theory[12] with $4f$ radial wave functions of Blume, Freeman, and Watson.[13]

2. The Approximate Low-Temperature Structure

According to the magnetic measurements, holmium undergoes a transition to a ferromagnetic state at approximately 20°K. However, in the absence of an applied field, only a small component of the magnetic moment parallel to the c axis participates in the ferromagnetism. The neutron evidence is shown in part in Fig. 3, where the intensities of a number of critical reflections, reduced to absolute $|F|^2$ values, are represented as functions of temperature. The satellites $(100)^+$ and $(000)^-$ increase in intensity with decreasing temperature and pass smoothly and continuously across the Curie point, and this suggests that a large component of the moment remains in the helical state. The normal nuclear reflections, with the important exception of (002) show a small but measurable increase in intensity at the Curie temperature. The existence of a magnetic contribution to the (110) reflection requires that the magnetic configuration have a net magnetic moment. The absence of a magnetic contribution to (002) requires that this moment be parallel to the c axis.

The magnetic configuration is therefore the conical, or the ferromagnetic spiral configuration in which

$$\begin{aligned}\mu_{nx}&=\mu\sin\gamma\cos(2\pi\boldsymbol{\tau}\cdot\mathbf{r}_n+\alpha),\\ \mu_{ny}&=\mu\sin\gamma\sin(2\pi\boldsymbol{\tau}\cdot\mathbf{r}_n+\alpha),\\ \mu_{nz}&=\cos\gamma.\end{aligned}\tag{3}$$

The structure factors for the satellites are given by Eq. (2) with μ replaced by $\mu\sin\gamma$: The constant component parallel to the c axis puts magnetic intensity into the normal nuclear positions according to the relation

$$|F|_{hkl}^2=0.0725\mu^2\cos^2\gamma f^2|G|_{hkl}^2q^2\tag{4}$$

in which γ is the semi-apex angle of the cone and q is the magnitude of the magnetic interaction vector ($q^2=\sin^2\phi$, where ϕ is the angle between the moment direction, the c axis in this case, and the scattering vector).

In Table II are summarized the observed and calculated intensities for the 4.2°K data obtained from

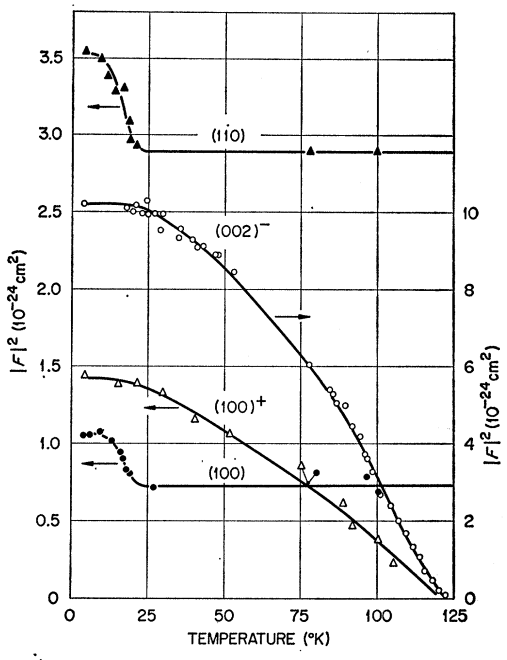

Temperature Variation of Reflections from Holmium.

FIG. 3. Temperature variation of magnetic reflections of holmium. The scale to the right applies to $(002)^-$. The increase in intensity of the (100) and (110) reflections indicates a ferromagnetic component below about 20°K.

[11] W. C. Koehler, E. O. Wollan, and M. K. Wilkinson, Phys. Rev. **110**, 37 (1958).
[12] G. T. Trammell, Phys. Rev. **92**, 1387 (1953).
[13] M. Blume, A. J. Freeman, and R. E. Watson, J. Chem. Phys. **37**, 1245 (1962). An arithmetic error occurs in the computation of the theoretical curve of Fig. 2 in this paper. The agreement between theory and experiment is much better than indicated there.

TABLE II. Intensities of magnetic reflections of Ho at 4.2°K. The observed $|F|^2$ values (units of 10^{-24} cm²) are averaged over equivalent reflections. The calculated values yield $\mu = (9.5\pm0.3)\mu_B$, $\mu_z = (2.1\pm0.05)\mu_B$.

Reflection[a]	$\|F\|_{obs}^2$ (10^{-24} cm²)	$\|F\|_{calc}^2$ [b]	Reflection[a]	$\|F\|_{obs}^2$	$\|F\|_{calc}^2$ [c]
$(100)^-$	1.44±0.08	1.34	(100)	0.311±0.05	0.261
$(100)^+$	1.44±0.08	1.34	(002)	0.00 +0.14	0.00
$(101)^-$	4.22±0.24	4.45	(101)	0.455±0.13	0.642
$(101)^+$	4.22±0.24	4.72	(102)	0.144±0.04	0.134
$(\bar{1}01)^-$	4.20±0.24	4.45	(110)	0.660±0.17	0.656
$(\bar{1}01)^+$	4.28±0.24	4.72	(112)	0.419±0.16	0.412
$(102)^-$	1.68±0.09	1.60			
$(102)^+$	1.70±0.09	1.53			
$(002)^-$	10.3 ±0.58	10.7			
$(002)^+$	9.06±0.54	9.6			
$(110)^-$	3.47±0.20	3.40			
$(110)^+$	3.42±0.20	3.40			
$(112)^-$	3.52±0.20	3.30			
$(112)^+$	3.00±0.17	3.07			
$(\bar{1}\bar{1}2)^-$	3.49±0.20	3.30			
$(\bar{1}\bar{1}2)^+$	2.98±0.17	3.07			

[a] Averaged over equivalent reflections.
[b] $\langle p^2\rangle = 6.52\pm0.37$, $\mu = (9.5\pm0.3)\mu_B$.
[c] $\langle p^2\rangle = 0.32\pm0.05$, $\mu_z = (2.10\pm0.05)\mu_B$.

Ho(A).[14] The agreement for the spiral contributions is again quite satisfactory. For the "ferromagnetic" reflections it is somewhat worse because small magnetic intensities are superimposed upon larger nuclear ones.

3. Temperature Variation of the Modulation Wave Vector

The wave vector τ was measured at various temperatures, usually from the angular separation of the magnetic satellites of a (100) reflection. Since the spacings for (100) and $(100)^\pm$ are very nearly the same, the counter could be fixed at the appropriate scattering angle and the crystal rocked to record successively the reflections $(100)^-$, (100), $(100)^+$ as shown in Fig. 1. A typical angular separation of the satellites was 17°.

The results of the measurements are summarized in Fig. 4, and we have included results for both crystals because it is in these measurements that significant differences appear. Thermal hysteresis was observed for Ho(B) in the vicinity of 20°K, but in the higher temperature range no significant differences in data obtained on warming and on cooling were noted. Both crystals showed an initial value of the turn angle, measured just below the Néel point, of about 50° per layer. In both cases the turn angle decreases with decreasing temperature. In Ho(A), it becomes constant at a value of 36.7° per layer at a temperature near 35°K. For Ho(B) the turn angle reaches a value of precisely 30° per layer below about 19°K.

Some significant parameters for the two crystals are summarized in tabular form in the figure. The Néel points differ by 11°K, but within experimental error the Curie points are identical. With a minimum value of ω equal to 30.0° the magnetic cell for Ho(B) is commensurable with the chemical cell ($\tau = b_3/6$). The temperature, measured on warming, at which ω departs from its minimum value T_ω is about 35°K for Ho(A); for Ho(B) it is at the Curie point, within the error of observation.

4. The Low-Temperature Structure

(a) *Description of the Observations*

In a preceding paragraph we have described the approximate low-temperature structure of holmium as a ferromagnetic spiral configuration. The term approximate has been used because there are in the diffraction patterns weak, but measurable, magnetic reflections of the type (00l) which correspond to higher harmonics of the strong, primary satellites. Such higher harmonics were observed for both crystals, but, since the values of τ at 4.2°K are different in the two cases, the disposition of the higher order reflections is different also. For Ho(A) the extra reflections were very much weaker than in Ho(B) and the conical configuration is a very good approximation indeed. Accordingly, we deal here only with data for Ho(B).

A representative set of data obtained in a slow scan with counter and crystal coupled is shown in Fig. 5. A background correction, obtained with the crystal turned several degrees off the Bragg reflecting position has been subtracted off.

The indexing is indicated in the figure by the integers above the several peaks and these are to be taken as the corresponding multiples of $\frac{1}{6}$, the appropriate fraction for the observed wave vector at 4.2°K. The first, very strong line in the pattern, is the primary or fundamental satellite of the origin $(000)^{+1}$; the line labeled 11, is the corresponding fundamental harmonic of (002). The others may be regarded as higher har-

[14] Analysis of the data for the two crystals, A and B, gave values of $2.1\mu_B$ and $1.7\mu_B$, respectively, for the c-axis component of the moment. The basal-plane component was $9.5\mu_B$ in each case.

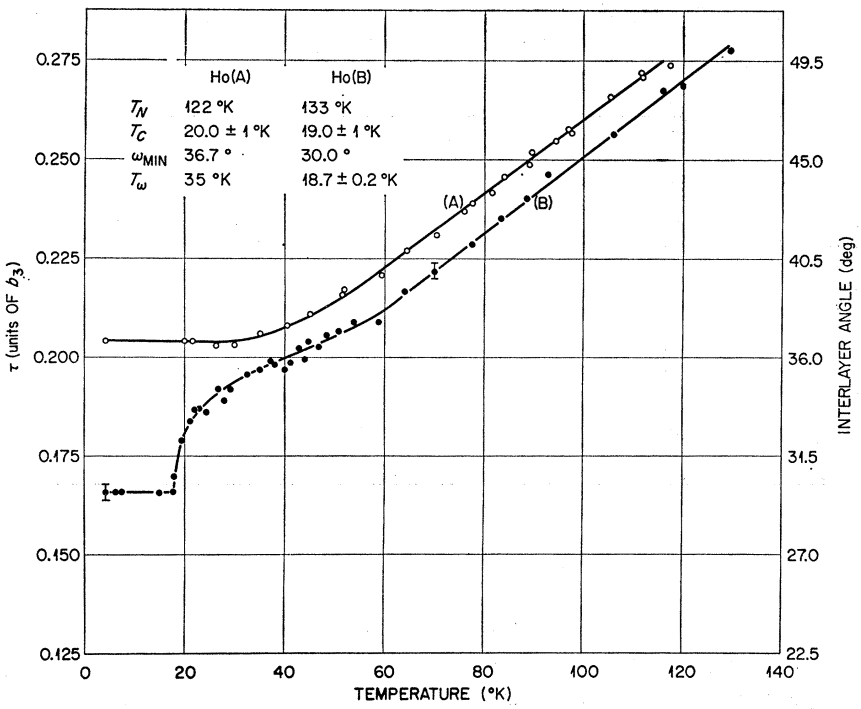

FIG. 4. Temperature variation of wave number of holmium crystals. The scale on the left is the wave number in units of b_3; that on the right the corresponding interlayer angle. Pertinent data characteristic of the two crystals are collected in the insert.

monics of these; for example, 2 corresponds to $(000)^{+2}$, and 7 to $(002)^{-5}$.

In the particular set of data shown in the figure there is no line at the position of $(002)^{-2}$ (at position 10), nor are there lines corresponding to third harmonics (3, and 9). There is, however, a contribution to (001) much too great to be attributed to residual second-order contamination of the filtered incident beam.

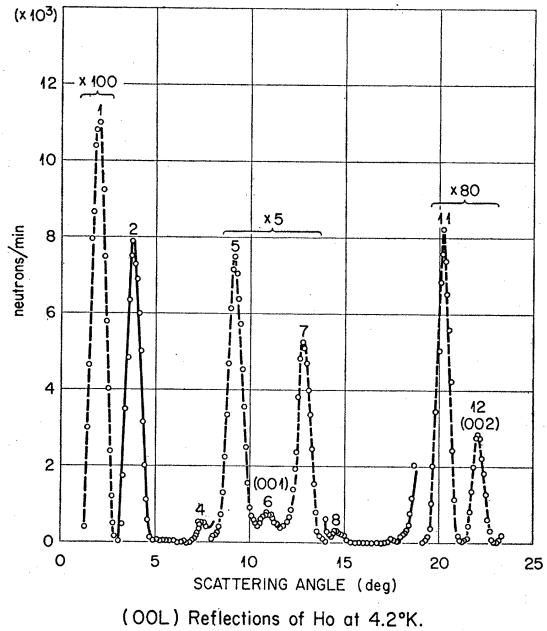

FIG. 5. Reflections (00L) for Ho at 4.2°K. For the particular azimuthal orientation of the crystal in the experiment no line corresponding to the second harmonic of (002) is observed. Note changes in scale.

With another orientation of the sample about its c axis, a peak at the second harmonic position $(002)^{-2}$ was observed. Changes in the relative intensities of some of the other reflections were observed as well.

It is well known that "forbidden" reflections may be observed when the geometrical relationships for simultaneous Bragg scattering are satisfied.[15,16] In order to ascertain which if any of the higher harmonics was due to a real distortion of the helical configuration of moments in the basal plane, a Renninger-type experiment was carried out for each of them. The counter was fixed at each of the positions 2 through 10, the crystal adjusted for Bragg reflection, and then rotated about the c axis. Because of the symmetry of the crystal a 30° rotation was sufficient. With the exception of $(000)^{+2}$ all reflections except 5 and 7 were proved in these experiments to be Renninger peaks and hence not associated with distortions of the magnetic structure.

The reality or nonreality of the second harmonic of the origin has been more difficult to demonstrate. At the neutron wavelengths customarily used the strong primary harmonic of the origin is found at a scattering angle of about 2°, and the second harmonic, accordingly, is at 4° from the direct beam. Severe collimation was

[15] M. Renninger, Z. Physik **106**, 141 (1937).

[16] R. M. Moon and C. G. Shull, Acta Cryst. **17**, 805 (1964). See also G. Borgonovi and C. Caglioti, Nuovo Cimento **24**, 1174 (1962). H. J. Hay, Atomic Energy Research Establishment Report No. R-2982, Harwell, Berkshire, England, 1959 (unpublished).

TABLE III. Analytic expression for $|G'|_{HKL}^2$ for the double cone and bunched spin models for Ho at 4.2°K. Where necessary averages over domains have been taken. The reflections (006) and (00,12) have zero intensity because the moment and scattering vector appropriate to them are parallel. The entries in the table are referred to one unit chemical cell.

Index	Double cone	Bunched spin
001 (00,11)	$(\sin\gamma_e+\sin\gamma_o)^2$	$\sin^2\gamma(2+2\cos(2\pi/12-2\delta))$
005 (007)	$(\sin\gamma_e-\sin\gamma_o)^2$	$\sin^2\gamma(2-2\cos(2\pi/12-2\delta))$
101 (10,11)	$(\sin\gamma_e-\sin\gamma_o)^2+\sin\gamma_e\sin\gamma_o$	$\sin^2\gamma(2-\cos(2\pi/12-2\delta))$
105 (107)	$(\sin\gamma_e+\sin\gamma_o)^2-\sin\gamma_e\sin\gamma_o$	$\sin^2\gamma(2+\cos(2\pi/12-2\delta))$
111 (11,11)	$(\sin\gamma_e+\sin\gamma_o)^2$	$\sin^2\gamma(2+2\cos(2\pi/12-2\delta))$
115 (11,7)	$(\sin\gamma_e-\sin\gamma_o)^2$	$\sin^2\gamma(2-2\cos(2\pi/12-2\delta))$
006	$(\cos\gamma_e-\cos\gamma_o)^2$	0
0012	$(\cos\gamma_e+\cos\gamma_o)^2$	$4\cos^2\gamma$
100 (11,12)	$(\cos\gamma_e-\cos\gamma_o)^2+\cos\gamma_e\cos\gamma_o$	$\cos^2\gamma$
106	$(\cos\gamma_e+\cos\gamma_o)^2-\cos\gamma_e\cos\gamma_o$	$3\cos^2\gamma$
110 (11,12)	$(\cos\gamma_e+\cos\gamma_o)^2$	$4\cos^2\gamma$
116	$(\cos\gamma_e-\cos\gamma_o)^2$	0

used in order to achieve sufficient resolution. Nevertheless in most experiments the $(000)^{\pm1}$ spots were sufficiently diffuse that the sphere of reflection could conceivably pass simultaneously through (for different domains) the + and − satellites of the origin and so give rise to an apparent second harmonic. The intensity of a line so produced would be independent of azimuth angle.

That the second harmonic is due in part to double scattering is indicated by the results of measurements on pillar-shaped crystals, which gave different relative intensities for the second and first harmonics, and by the different relative intensities obtained with a given crystal in different geometries, and at different wavelengths. Under the most severe conditions, the intensity of the second harmonic at 4.2°K could be reduced to about 0.3% of the first but it could never be eliminated completely. Inasmuch as the second harmonic of (002) was definitely spurious, a real second harmonic of the origin would have to be due to a spin density distribution different from that of the f electrons. From the experimental point of view it appears that the second harmonic of the origin is due to causes other than a distortion of the configuration of moments.

(b) *Models for the Structures*

The existence of real fifth and seventh harmonics in the diffraction patterns at 4.2°K is evidence that the basal-plane configuration is different from the ideal helical arrangement. It is known from low-temperature-magnetization studies that the a directions are very hard directions of magnetization; it is therefore reasonable to attribute the distortion to the hexagonal anisotropy energy.

The hexagonal anisotropy energy per atom in the classical approximation is proportional to $\sin^6\gamma\cos6\phi$ where γ, and ϕ are polar coordinates of the moment in question and the constant of proportionality is positive (for Ho^{+3}) if ϕ is measured from one of the hexagonal axes (a directions) in the plane of the layer. With a wave vector corresponding to precisely 30°, the moments would tend to fall alternately in easy and hard directions, an energetically unfavorable situation. The potential energy can be conveniently minimized in the two ways illustrated in Fig. 6.[17] Both of these models are distortions of the simple conical arrangement which produce fifth and seventh harmonics, and no others, and we shall consider them in some detail.

In the model of Fig. 6(a) the moments fall alternately on the surfaces of cones of different angular opening so that the projections of the moments on the basal plane, Fig. 6(b), are alternately long and short. At least one cone is required because of the spontaneous magnetization along the c axis. In the model we consider here the moments deviate from the surface of this cone, thus producing two, such that as $\cos6\phi=+1$, $\sin\gamma$ is reduced

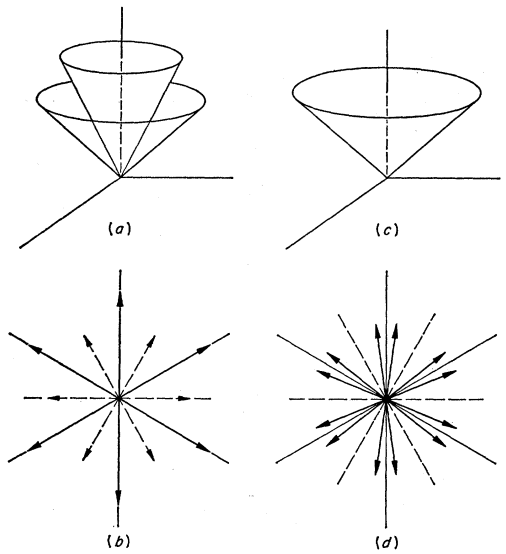

FIG. 6. Representations of possible models for the low-temperature virgin-state magnetic structure of holmium (B). The moments are all supposed to be referred to a common origin. In the double-cone model (a), the moments make alternately a long and a short projection on the basal plane (b). In the bunching model, there is a single cone (c), but the projections on the plane are alternately close together and far apart (d).

[17] We are much indebted to Professor T. Nagamiya for discussions concerning these models.

and where $\cos 6\phi = -1$, $\sin\gamma$ is increased. The spontaneous moment is then the mean value of the projection of the moments on the c axis.

In the second model, Fig. 6(c) and 6(d), it is assumed that the same value of γ applies to all moments, but the crests of potential energy are avoided by bunching the moments symmetrically about the b directions which are the easy directions of magnetization. The spontaneous moment is determined by the single cone angle γ.

Since we are considering the case in which the magnetic unit cell is precisely six times as long, in the c direction, as the chemical cell it will be convenient to refer the indices of the magnetic reflections to that cell. On the same basis, the atoms are located, on the even layers, in the positions $(0, 0, 0+\frac{1}{6}n)$, and on the odd layers in $(\frac{1}{3}, \frac{2}{3}, \frac{1}{12}+\frac{1}{6}n)$, where n is an integer which takes on values from zero to five, inclusive.

The magnetic structure of the double-cone model will be given by[18]

$$\begin{aligned} &\mu_{nx}{}^{e}=\mu\sin\gamma_e\cos\frac{2\pi n}{6}, \quad &&\mu_{nx}{}^{o}=\mu\sin\gamma_o\cos 2\pi\left(\frac{n}{6}+\frac{1}{12}\right),\\ &\mu_{ny}{}^{e}=\mu\sin\gamma_e\sin\frac{2\pi n}{6}, \quad &&\mu_{ny}{}^{o}=\mu\sin\gamma_o\sin 2\pi\left(\frac{n}{6}+\frac{1}{12}\right),\\ &\mu_{nz}{}^{e}=\mu\cos\gamma_e, &&\mu_{nz}{}^{o}=\mu\cos\gamma_o, \end{aligned} \tag{5}$$

where now e and o refer to the even and odd layers.

The "bunched moment" model may be described by

$$\begin{aligned} &\mu_{nx}{}^{e}=\mu\sin\gamma\cos\left(2\pi\frac{n}{6}-\delta\right), \quad &&\mu_{nx}{}^{o}=\mu\sin\gamma\cos\left(2\pi\frac{n}{6}+\delta\right),\\ &\mu_{ny}{}^{e}=\mu\sin\gamma\sin\left(2\pi\frac{n}{6}-\delta\right), \quad &&\mu_{ny}{}^{o}=\mu\sin\gamma\sin\left(2\pi\frac{n}{6}+\delta\right),\\ &\mu_{nz}{}^{e}=\mu\cos\gamma, &&\mu_{nz}{}^{o}=\mu\cos\gamma. \end{aligned} \tag{6}$$

Moments in adjacent layers are thus alternately close together, angular separation 2δ, and far apart, $60-2\delta$.

The intensities to be expected from these two models are readily calculated and can be put into a form similar to that of Eq. (4)

$$\begin{aligned} &|F|_{HKL}{}^{2}=0.0725\mu^2 f^2\frac{(1+\cos^2\phi)}{4}|G'|_{HKL}{}^{2}, \quad L=1, 5, 7, 11, \cdots,\\ &|F|_{HKL}{}^{2}=0.0725\mu^2 f^2\sin^2\phi|G'|_{HKL}{}^{2}, \quad L=0, 6, 12, \cdots, \end{aligned} \tag{7}$$

where now the factor G' is somewhat more complicated than G. Analytical expressions for $|G'|_{HKL}$ for a few important and representative reflections are listed in Table III.

On the double-cone model, the intensities of primary satellite reflections ($00L$) are determined by the sum of the sines of the cone angle, of the higher harmonics by their difference. There is predicted a weak reflection at 116 (111 on the chemical cell) due to the difference of the c axis projections of the two sets of moments. It may be noted that if the two cone angles become equal to each other, the expressions listed in Table III reduce to those already set down for the ferromagnetic spiral.

From experiment the ratio $|G'|_{(005)}{}^{2}/|G'|_{(00,11)}{}^{2}$ was determined to be 0.029.[19] According to Table III, this value determines a relation between θ_e and θ_o. The spontaneous magnetization determines a second relation between the two angles such that $\frac{1}{2}(\cos\theta_e+\cos\theta_o)=\mu_f/\mu$, where μ_f is the ferromagnetic c-axis component.

In Fig. 7 are shown the sine and cosine relations so deduced. The curved line in the lower part of the figure is computed from the ratio of intensities of (005) and (00,11). To be consistent with the magnetization data the curve should intersect the one labeled $\mu_f=1.7$, but

[18] It will be noted that a definite relationship between the moment directions and crystal directions has been chosen in order to conform with the supposition that the hexagonal anisotropy energy is a governing factor in the determination of the structure.

[19] The density of (001) is much too high to be reliable.

it obviously does not do so. In order to intersect this curve the ratio of structure factors would have to be 0.0009, a value some 30 times smaller than observed. Even for $\mu_f=2.5\mu_B$, a value considered to be well outside the range of experimental error the maximum ratio is 0.0064 or about seven times smaller than observed. The double-cone model may therefore be eliminated from further consideration.

According to the second model we have selected, the angle δ ranges from 0° to 15°. For $\delta=0$ the moments are parallel in pairs to the easy directions; when $\delta=15°$ the expressions of Table I reduce to those deduced for the ferromagnetic spiral.[20]

As in the preceding model appeal is made to experiment to deduce the value of δ, and from the observed ratio of intensities of (005) and (00,11), δ is found to be 5.8°. Thus at 4.2°K the moments are alternately about 12° and 48° apart.

It appears that this configuration departs appreciably from the approximate structure. However, the intesities of the fundamental satellites are not particularly sensitive to such a distortion, and there is no further good check on the model. For the particular value of δ indicated, the squares of the geometrical parts of the structure factors of the main satellites are quite close to those calculated for the ferromagnetic spiral. Thus for example for (00,11) 3.89 as compared to 4.0; for (101) 1.05 compared to 1.0; for (105) 2.94 compared to 3.0. [The model does predict reflections (115) and (117) which are in fair agreement with experiment.] Moment values derived from the data on the assumption of a helical model are therefore subject to at most about a 2.5% correction.

(c) *The Structure at Intermediate Temperatures*

A number of measurements were carried out at various fixed temperatures above 4.2°K on the higher harmonics. As at 4.2°K it was necessary to carry out tedious measurements of intensity as a function of azimuth angle in order to establish which reflections were real, and which were due to double Bragg scattering.

Some results of this study are summarized in Fig. 8. Figure 8(*a*) reproduces a portion of the diffraction pattern observed at 4.2°K with a relatively large crystal. The fifth harmonics, a Renninger peak at (001), and residual second-order reflections are illustrated. (In this section the indexing is based on the chemical unit cell.) As the temperature was raised, the intensities of the higher harmonics remained essentially constant, as did the wave vector τ until near 19°K, the wave vector began to increase (Fig. 4), and the intensities to decrease. Figure 8(*b*) illustrates the same portion of the diffraction pattern at 21°K at which

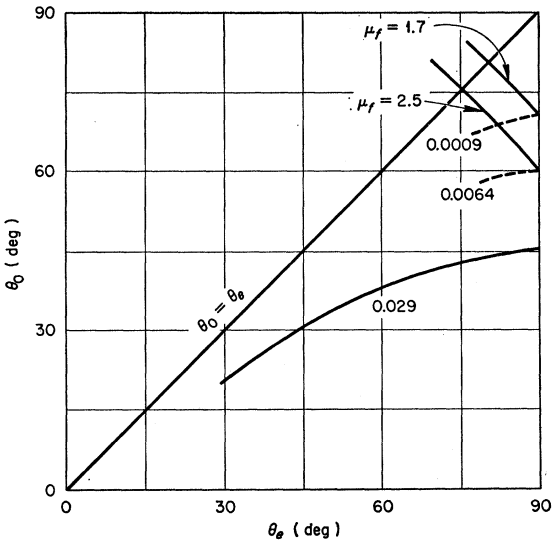

FIG. 7. Analysis of low-temperature data on the double-cone model. The lower curve is derived from expressions of Table III for the experimental ratio $|G'|_{(005)}^2/|G'|_{(00,11)}^2=0.029$. To be consistent with the magnetization data it should intersect the curve labeled $\mu_f=1.7$.

temperature the wave vector had reached a value of $0.183b_3$. In this case, since τ is no longer commensurable with the unit cell both the fifth and seventh harmonics may be seen since they are no longer superimposed. (Except for the second-order reflections all others are due to double Bragg scattering.) At still higher temperatures the intensities of the fifth and seventh harmonics dropped off still more until at about 40°K they were no longer observed. This is illustrated for $(000)^{+5}$ in Fig. 8(*c*).

For the crystal Ho(*A*), the intensity-temperature variation of $(000)^{+5}$ is as shown in Fig. 8(*d*). In this case, the turn angle remained constant to about 35°K and at that temperature the $(000)^{+5}$ reflection had fallen nearly to zero intensity. It will be recalled that the wave vector for Ho(*A*) was noncommensurable with the unit cell over the range of temperature studied.

Even in the more general case that the fundamental wave vector is incommensurable with the lattice, the hexagonal anisotropy energy will introduce fifth and seventh harmonics into the moment distribution, and into the diffraction patterns. It has been shown by Yosida[21] that the angle made by the moments in the nth layer with respect to those in some reference layer may be expressed as

$$\phi_n=(\phi_n)^0+h\sin 6(\phi_n)^0+\cdots, \qquad (8)$$

where $(\phi_n)^0=2\pi\boldsymbol{\tau}\cdot\mathbf{r}_n+\alpha$ is the corresponding angle in the absence of anisotropy and α is some phase angle.

[20] In the expression for (*H*0*L*) reflections, an average over domains has been taken.

[21] See for example K. Yosida, in *Progress in Low Temperature Physics IV*, edited by C. J. Gorter (North-Holland Publishing Company, Amsterdam, 1964), p. 265.

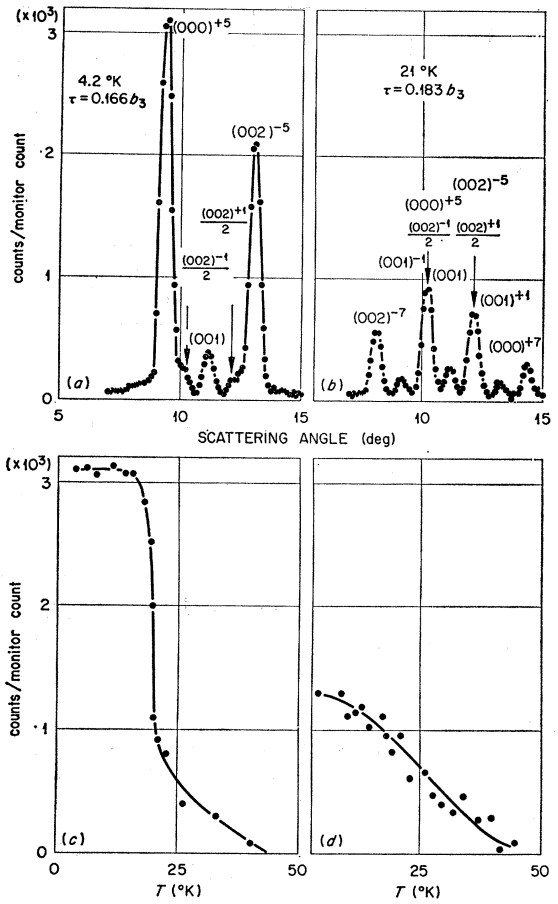

FIG. 8. The higher harmonics. (*a*) Ho(*B*) at 4.2°K. The $(000)^{+5}$ and $(002)^{-7}$ are at positions corresponding to a magnetic unit cell whose *c* axis is six times as long as that of the chemical cell. For the particular azimuthal angle of the experiment an apparent (001) reflection is observed. Under the conditions of the experiment weak second-order reflections $(002)^{\pm 1/2}$ are observed. (*b*) Ho(*B*) at 21°K. The magnetic unit cell is no longer simply commensurable with the chemical cell and both fifth and seventh harmonics are found. The reflections indexed as $(001)^{\pm}$ are spurious. (*c*) Temperature variation of intensity of $(000)^{+5}$ for Ho(*B*). (*d*) Temperature variation of intensity $(000)^{+5}$ for Ho(*A*).

The coefficient h is proportional to the hexagonal anisotropy energy.

The structure factors for a distribution of moments described by

$$\begin{aligned}\mu_{nx}&=\mu\cos\phi_n,\\ \mu_{ny}&=\mu\sin\phi_n,\\ \mu_{nz}&=0,\end{aligned}\qquad(9)$$

with ϕ_n given above may readily be calculated by an extension of a method suggested in an earlier paper.[22] In general, the reflections which will occur are the primary satellites $(HKL)^{\pm 1}$, and those corresponding to fifth and seventh, eleventh and thirteenth, etc., harmonics, and their $|F|^2$ values are

$$\begin{aligned}|F|^2=0.0725\mu^2 f^2\frac{(1+\cos^2\phi)}{4}|G|_{HKL}^2\\ \times J_0^2(h)\quad (HKL)^{\pm 1}\\ \times J_1^2(h)\quad (HKL)^{\pm 5,\pm 7}\\ \times J_2^2(h)\quad (HKL)^{\pm 11,\pm 13}\\ \text{etc.}\end{aligned}\qquad(10)$$

where $J_n(h)$ is the nth order Bessel function of argument h and G_{HKL} is the usual geometrical structure factor. As long as h is small $J_2^2(h)$ is negligible compared to $J_1^2(h)$ and only the primary, and fifth and seventh harmonics will be observed.

It should be emphasized that the low-temperature case illustrated in Fig. 8(*a*) is degenerate in the sense that the fifth and seventh harmonics of (000) and (002) superimpose. As soon as the degeneracy is removed, both sets of harmonics, as in Fig. 8(*b*), will be observed.

The temperature variation of the intensity of the fifth harmonic, as shown in Fig. 8(*c*) and 8(*d*) is to be attributed in part to the temperature variation of the hexagonal anisotropy energy. Its effect persists to surprisingly high temperatures.[23]

DISCUSSION

The theory of magnetism in the rare-earth metals has been reviewed recently by Elliott,[24] Nagamiya,[25] and Yosida.[21] It is generally accepted that the rare-earth atoms in the metals behave as tripositive ions the moments of which are coupled by indirect exchange interactions of the Ruderman-Kittel-Kasuya-Yosida type. The oscillatory character of the magnetic structures is a consequence of the long-range oscillatory nature of the interaction. When this interaction is applied to a hexagonal-close-packed system with three free conduction electrons per atom it is found that the wave vector for minimum free energy is about 50° per layer in remarkable agreement with the value observed for holmium near its Néel point. Recent work[26] on the Fermi surfaces of rare-earth metals has shown, however, that they are far from spherical, and it appears that the agreement cited above is somewhat fortuitous.

The several modifications of structures found in the rare earths depend upon anisotropy energy, an important source of which is the crystalline field, but the effect of anisotropic exchange must also be considered.[27]

[22] W. C. Koehler, Acta Cryst. **14**, 535 (1961).

[23] As will be seen in a second paper on the magnetization process in Ho, the hexagonal anisotropy manifests itself in making the *a* direction a hard direction of magnetization to comparably high temperatures.

[24] R. J. Elliott, in *Magnetism IIA*, edited by G. T. Rado and H. Suhl (Academic Press Inc., New York, 1965), p. 385.

[25] T. Nagamiya, J. Appl. Phys. Suppl. **33**, 1029 (1962).

[26] J. O. Dimmoch and A. J. Freeman, Phys. Rev. Letters **13**, 750 (1964). R. W. Williams, T. L. Louchs, and A. R. Mackintosh, *ibid.* **16**, 168 (1966).

[27] T. A. Kaplan and D. H. Lyons, Phys. Rev. **129**, 2072 (1963). See also F. Specht, Phys. Rev. (to be published).

The crystal-field anisotropy energy, for a single ion may be expressed, in the notation of Miwa and Yosida[28] as

$$E_a = DP_2(\cos\theta) + EP_4(\cos\theta) + FP_6(\cos\theta) + G\sin^6\theta\cos 6\phi, \quad (11)$$

where θ and ϕ, measured from the c axis and an a axis respectively are the spherical polar coordinates for the moment vector J of a given atom and $P_n(\cos\theta)$ is the Legendre polynomial of order n. The signs of the coefficients in Eq. (11) have been estimated on the assumption of tripositive ions at nearest-neighbor positions and neglect of more distant neighbors of a given atom. For holmium the sequence is $+$, $+$, $-$, for D, E, F, respectively. The sign of G is positive, as we have indicated above. A rough estimate of the magnitudes of the coefficients has been obtained also. More important, however, the theory[29] predicts that the axial anisotropy energy described by a spherical harmonic of order n varies with the relative magnetization M_r as M_r to the power $\frac{1}{2}n(n+1)$ and the hexagonal anisotropy energy as $M_r{}^6$. The several terms in Eq. (11) should therefore be strongly temperature-dependent with the second-order term $DP_2(\cos\theta)$ being the most important at higher temperatures. The experimental results appear to be in accord with the above remarks.

In Ho^{+3}, the total 4-f charge distribution is slightly flattened in a direction parallel to the total angular momentum J (the quadrupole moment is negative). The positive sign for D implies a minimum of potential energy ($P_2(\cos\theta)=\frac{1}{2}(3\cos^2\theta-1)$) if the moments are parallel to the basal plane, and this is consistent with an orientation of the charge distribution which places negative charge density nearer the close out-of-plane point charges than to the more distant in-the-plane neighbors.[30]

As long as the dominant term in the axial anisotropy energy is the second-order term, the moments are expected to lie in the basal plane and they are observed to do so to a temperature of about 20°K. At lower temperatures the higher order terms may become important. If only the fourth-order energy be considered, the moments will stay in the basal plane so long as $E<0.4D$. For $E>0.4D$ a minimum of potential energy is achieved if $\cos^2\theta=3/7(1-0.4D/E)$ instead of $\theta=\pi/2$. A conical configuration is therefore predicted. (If the sixth-order term is included as well, the cone angle is modified somewhat.)

From the experimental values of the cone angles in Ho(A) and Ho(B), 77.2° and 80.9°, respectively, one obtains from the above condition ratios D/E of 2.21 and 2.35. Thus, at 4.2°K, the second- and fourth-order anisotropy energies are of the same order of magnitude.

The temperature dependence of the (100) and (110) reflections was illustrated for the temperature range below 20°K in Fig. 3. The appearance of the intensity-temperature curves implies that the development of the conical configuration is a second-order transition. Indeed, the curves in these figures may be taken to represent the temperature variation of the fourth-order anisotropy energy.

On theoretical grounds, the coefficient G is some 10–100 times smaller than D or E. Experimentally, however, the hexagonal anisotropy energy makes itself felt at much higher temperatures than the fourth-order axial term, both in the virgin state (persistence of the fifth and seventh harmonics) and in the ferromagnetic state (difficulty to turn the moments out of b directions).

ACKNOWLEDGMENTS

The authors wish to express their thanks to Professor F. H. Spedding, and Professor Sam Legvold of Iowa State University for making available to them the single-crystal and polycrystalline specimens of holmium used in this investigation.

APPENDIX: ON THE ORIGIN OF THE DIFFERENCES BETWEEN DIFFERENT SPECIMENS

The magnetic properties of the crystal Ho(B) appear to conform more closely to those reported from other types of measurements than those of Ho(A). In this section we report briefly on the attempts we have made to trace the origin of the difference in the two specimens.

Both crystal specimens had been obtained from metal produced at Ames and it was expected that both would be of the highest purity possible. Nevertheless, since the Ho(A) metal had been produced prior to 1959 and the Ho(B) somewhat later, a complete quantitative analysis for other rare earths and yttrium, and a semi-quantitative analysis for other metallic impurities was made spectroscopically. According to the results of the analysis the two metals were indistinguishable and contained less than 0.01% Lu, Yb, and Y; less than 0.05% Er, Tm, Tb, Gd, Eu, and La, and less than 0.1% Ce, Pr, Nd, Sy, and Dy. Other metallic impurities if present were in amounts less than the limits of detection (0.05%).

A vacuum-fusion analysis was carried out on a fragment of the Ho(A) crystal to ascertain if an inordinately high percentage of oxygen was present. The result, 0.28%, by weight appears not to be dissimilar from the oxygen content of metal presently available commercially.

To check further on the influence of oxygen impurity on the properties of holmium, a series of polycrystalline specimens obtained from different vendors, at different times, and with known oxygen content, were investigated. A few variations in mechanical history were made also. The interlayer turn angle at 4.2°K was taken

[28] H. Miwa and K. Yosida, Progr. Theoret. Phys. (Kyoto) **26**, 693 (1961).

[29] See for example R. J. Elliott, Phys. Rev. **124**, 346 (1961).

[30] As pointed out by Trammell and quoted by Elliott the second-order anisotropy energy would vanish if the c/a ratio were the ideal value 1.633. In Ho the value of this ratio is considerably smaller than the ideal value.

as the criterion, and this was measured from the strong satellites of the origin. For Ho(A) the angular separation of the two satellites at 1.093 Å was 4.54°, and for Ho(B), 3.71°, and the resolution was such that the two values could easily be distinguished.

A first sample of doubly distilled high-purity holmium containing 0.17% O_2 was studied in the form of massive pieces broken from the bulk specimen. A value of $\omega=30.7°$ was obtained at 4.2°K. A second sample of ordinary commercial 99+% metal, also containing 0.17% O_2 was studied in the form of unannealed filings. The lines were slightly broadened in comparison to those from the high-purity specimen. A value for $\omega=30.3°$ was deduced. The third powder sample was of commercial Ho in the form of filings and "sawdust" which had been in the laboratory in an unsealed container for over four years. This should have been a good sample of poor metal, but it too yielded a value of $\omega=30.6°$ at low temperatures. The three powder samples, as well as the other two single crystals Ho(C) and Ho(D) all had values of ω_f equal, within experimental error, to that of Ho(B).

It appeared that the unique behavior of Ho(A) could not be attributed to impurities in the metal, and a second possibility related to the manner of formation of the crystals was considered. The crystals Ho(B), Ho(C), and Ho(D) were all grown by a strain-anneal method whereas Ho(A) was cut from an as-cast, machined rod. Short of the obvious experiment of annealing Ho(A) (we are reluctant to risk losing a crystal which is by chance "frozen in" at a final turn angle of 36.7°) we have tried to study the effects of mechanical history by studying severely cold-worked polycrystalline specimens. It is not certain that the cold-worked state is necessarily equivalent to the as-cast condition of Ho(A), but in any case no effects of cold work on the final turn angle were observed. We still have no explanation for the properties of Ho(A).

PHYSICAL REVIEW VOLUME 151, NUMBER 2 11 NOVEMBER 1966

Quantum Oscillations of the Ultrasonic Absorption in Magnesium and Zinc*

E. W. Fenton† and S. B. Woods
Department of Physics, University of Alberta, Edmonton, Alberta, Canada
(Received 28 March 1966; revised manuscript received 11 May 1966)

Quantum oscillations of the ultrasonic absorption have been studied in magnesium and zinc at magnetic fields between 5 and 20 kG. Low-amplitude oscillations, similar to the de Haas–van Alphen oscillations of magnetic susceptibility in period, temperature dependence of the amplitude, and line shape, are observed when $ql\sim1$, where q is the propagation constant of the sound wave and l is the mean free path of the electrons. The dependence of the amplitude on the angle between the magnetic-field vector and the direction of sound propagation does not agree with predictions. Oscillations of much larger amplitude have been observed in zinc with $ql\sim15$. Difficulty arises in comparing measurements of these oscillations with theory because they are characteristic of a region intermediate between the de Haas–van Alphen and giant oscillation regimes. Spin splitting of the absorption peaks is observed in zinc, but not in magnesium.

INTRODUCTION

QUANTUM oscillations of the acoustic-attenuation coefficient which are periodic in the reciprocal of the applied magnetic field have been observed in bismuth,[1–3] zinc,[4,5] antimony,[6] and gallium.[7] The phenomena are observed at high magnetic fields and are of two types: oscillations similar to de Haas–van Alphen oscillations in the magnetic susceptibility, and "giant quantum oscillations," which are a large amplitude resonance effect in the electron-phonon interaction. The factors determining which oscillations are observed are the sound frequency and mean free path of the electrons. de Haas–van Alphen oscillations occur when the frequency is low and the mean free path is short, and giant oscillations occur if the frequency is high and the mean free path is very long.

Although phenomena observed in bismuth, zinc, and gallium have been described in the literature as giant quantum oscillations, the electron mean free path must be nearly a centimeter for this effect, and only in gallium has this requirement been clearly satisfied. Close examination of magnetoacoustic oscillations reported in bismuth and zinc reveals that they are characteristic of some regime intermediate between the de Haas–van Alphen and giant quantum oscillation

* This work was supported by the National Research Council of Canada.
† Present address: Department of Physics, Simon Fraser University, Burnaby 2, British Columbia, Canada.
[1] D. H. Reneker, Phys. Rev. **115**, 303 (1959).
[2] J. G. Mavroides, B. Lax, K. J. Button, and Y. Shapira, Phys. Rev. Letters **9**, 451 (1962).
[3] A. M. Toxen and S. Tansal, Phys. Rev. **137**, A211 (1965).
[4] D. Gibbons, Phil. Mag. **6**, 445 (1961).
[5] A. P. Korolyuk and T. A. Prushchak, Zh. Eksperim i Teor. Fiz. **41**, 1689 (1961) [English transl.: Soviet Phys.—JETP **14**, 1201 (1962)].
[6] J. B. Ketterson, Phys. Rev. **129**, 18 (1963).
[7] Y. Shapira and B. Lax, Phys. Rev. **138**, A1191 (1965).